Journal of the European Ceramic Society **15** (1995) 225–232
Elsevier Science Limited
Printed in Great Britain
0955-2219/95/$9.50

Properties and Interface Structures of Ni and Ni–Ti Alloy Toughened Al_2O_3 Ceramic Composites

X. Zhang,[a] G. Lu,[b] M. J. Hoffmann[c] & R. Metselaar[a]

[a]Centre for Technical Ceramics, Eindhoven University of Technology, Eindhoven, The Netherlands
[b]Max-Plank-Institut für Metallforschung, Institut für Physik, Stuttgart, Germany
[c]Max-Plank-Institut für Metallforschung, Institut für Werkstoffwissenschaften, Pulver-metallurgisches Laboratorium, Stuttgart, Germany

(Received 8 February 1994; revised version received 20 June 1994; accepted 1 August 1994)

Abstract

Ni/Al_2O_3 and $Ni–Ti/Al_2O_3$ composites sintered in different atmospheres are investigated. Argon as a sintering atmosphere is found to be more beneficial to the fracture toughness of the composites than CO. Ni inclusions at 12 vol.% enhance the fracture toughness up to 36%, corresponding to a fracture energy twice that of the alumina matrix, whereas titanium alloying to Ni makes a negative contribution to the mechanical behaviour. The interfacial structures of Ni/Al_2O_3 and $Ni–Ti/Al_2O_3$ are studied by using electron microscopy. The titanium distribution at the interfaces is studied and correlated to the mechanical properties.

1 Introduction

Brittle ceramic materials can be toughened by the incorporation of ductile reinforcements. The toughening mechanism has already been investigated both theoretically and experimentally.[1–4] The plastic stretching of ductile reinforcements accounts for the predominant toughening. For effective toughening the appropriate interface bonding strength is the first requirement. If the bonding strength is too weak, cracks will propagate along the interface and plastic stretching of the ductile reinforcements will not occur. This is the usual case for many metal/ceramic composites. If the bonding strength is too strong, a rare case, the plastic stretching will be only localized to a limited zone between surfaces of propagating cracks and the toughness of the reinforcements will not be utilized adequately.[5] Therefore, in a metal reinforced ceramic composite, the fracture toughness can be enhanced by optimizing the metal/ceramic interface behaviour, which depends on both the physical properties (such as morphology, elastic modulus, thermal expansion coefficient) and the chemical characters of each material.

As a model system, Ni particle toughened Al_2O_3 has been studied.[6,7] A large increase in fracture toughness has been reported for Ni/Al_2O_3 composites compared to that of the monolithic alumina matrix. However, it seems that the potential for toughening is not fully reached because the plastic stretching of the Ni particles is limited. Cracks propagate often around the Ni particles, i.e. along the Ni/Al_2O_3 interfaces, owing to the low interface bonding strength as compared to the high yielding strength of Ni. Therefore, in order to get a well-toughened composite, the interface bonding between Ni and Al_2O_3 should be strengthened.

The common practice for interface strength adjustment is to introduce a degree of interfacial chemical reaction. In preparing composite materials, this can be achieved either by controlling the sintering atmosphere or by introducing additives. As far as the atmosphere is concerned, Ni can be oxidized to form a NiO or a $NiAl_2O_4$ spinel interlayer. As to additives, titanium is widely used as a wetting agent in brazing ceramics with alloys to achieve strong joints.[8] It has been reported that the interface energy between Ni and sapphire (or sintered Al_2O_3) decreases sharply on the addition of a small amount (about 2%) of Ti in Ni because of the segregation of Ti and the formation of Ti_2O_3 at the interface.[9] According to the concept of the work of adhesion, W_{ad}, defined as:

$$W_{ad} = \gamma_{Ni} + \gamma_{Al_2O_3} - \gamma_{Ni/Al_2O_3}$$

the interface bonding between Ni/Al_2O_3 can be improved by the presence of Ti. In the present work, pure Ni and Ni–Ti alloy toughened Al_2O_3 composites are prepared by sintering in either Ar

Table 1. Properties of the Ni(Ti)/Al_2O_3 composites

Sample	*Al_2O_3 (air)*	*1 12 vol%Ni (CO)*	*2 12 vol%Ni (Ar)*	*3 12 vol%Ni–Ti (CO)*	*4 12 vol%Ni–Ti (Ar)*
Density (%TD)	99·9	99·5	99·9	99·3	99·7
Strength (MPa)[a]	326 ± 24	196 ± 14	306 ± 13	180 ± 15	188 ± 10
K_{Ic} (MPa $m^{1/2}$)[a]	3·6	4·1	4·9	3·2	3·5

[a] Results of six measurements.

or CO atmospheres. The purpose is to investigate the influence of the atmospheres and of the titanium addition on the interface reactions and on the mechanical properties of the composites.

2 Experimental Procedures

The composites were prepared by a typical powder metallurgical route. Pure nickel powders (99·99 + %. ≤ 63 μm, Goodfellow) or Ni–Ti alloy powders (5 wt% or 6·06 at% Ti in Ni, prepared by an atomizer, sieved to under 63 μm) in the amount of 12 vol.% were mixed with fine Al_2O_3 powder (99·99% up, TM-DR, ultra pure sinterable alumina) in an attritor for 4 h with alumina balls and isopropanol as the milling media. The slurries were dried and sieved. Powder compacts with dimensions of about 13 × 21 × 57 mm were formed by cold isostatic pressing under a pressure of 625 MPa. The green compacts were sintered at 1400°C for 2 h in CO (generated by burning of carbon powder in a closed alumina crucible) and in Ar (static argon in an alumina tube furnace) respectively.

After sintering, the surfaces of the samples were carefully observed. The density was measured by the Archimedes method. Bending bars, 3 × 4 × 45 mm in size, were machined from the large sintered blocks. The mechanical testing was performed in the four-point-bending mode at a cross head speed of 0·1 mm/min. The strength was determined on the bending bars with inner/outer spans of 20/40 mm. The toughness was characterized on the subsequent half bars with inner/outer spans of 7/20 mm by the single-edge-notched-beam (SENB) method. The notch width was controlled to within 100 μm and the depth was about one fourth of the sample height, i.e. 1 mm.

The phases in the composites were examined by X-ray diffraction (XRD). The general morphology of the samples was studied with optical microscopy. The detailed structure of the interfaces was investigated by scanning electron microscopy (SEM) and transmission electron microscopy (TEM). The composition of the interfacial layers was determined by electron probe microanalysis (EPMA). Because of the uncertainties associated with analyzing oxygen content, quantitative analysis was only done on Ti, Ni and Al, using pure metals as the standards. To estimate the oxygen content, semi-quantitative (standardless) analysis was performed using energy dispersive spectroscopy (EDS) mode in SEM or TEM. Since the interfacial layers are generally very thin, analysis was always performed at places where the layers are relatively thick.

3 Results

3.1 Properties of the composites

The relative density, the fracture strength and toughness of the monolithic Al_2O_3 and of the composites are given in Table 1. All the samples were sintered nearly to their theoretical densities in the different atmospheres by normal sintering. The composites have lower fracture strength than monolithic Al_2O_3. The Ni/Al_2O_3 composites have improved fracture toughness with an increase of 14 and 36% over Al_2O_3 in the case of CO and Ar as the sintering atmospheres, respectively. Calculation from the toughness shows that the fracture energy ($\gamma = K_{Ic}^2/2E$) of Al_2O_3 and of sample 2 are 16·8 J/m^2 and 32·9 J/m^2, namely a doubling of the fracture energy in the composite as compared with the pure matrix material. For the Ni–Ti/Al_2O_3 composites, a decrease in fracture toughness is found with either CO or Ar as the sintering atmosphere. These results suggest that the atmospheres have a large influence on the fracture properties of the composites, and that an Ar atmosphere is more beneficial than a CO atmosphere. The addition of Ti to Ni produces no improvement in toughening.

3.2 Microstructures and interfaces

The appearance of all the sintered composites is more or less yellow-green, but with one surface blue, which was in contact with the alumina crucible during sintering. XRD analyses reveal that the yellow-green surfaces contain NiO and the blue ones $NiAl_2O_4$ spinel. After removing the surface scales, which are thinner than 0·5 μm, the samples

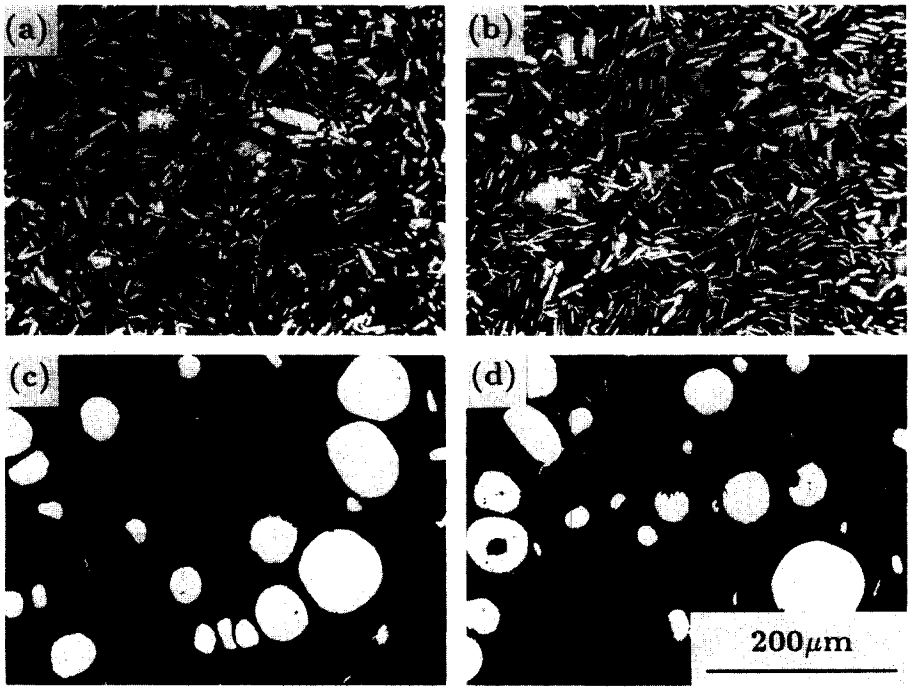

Fig. 1. Optical micrographs of the samples: (a) 1, (b) 2, (c) 3 and (d) 4.

appear dark grey for the Ni/Al_2O_3 composites and grey for the Ni–Ti/Al_2O_3 composites. No other phases except Ni (Ni–Ti) and Al_2O_3 can be detected by XRD. Since we are interested in the bulk properties of the composites, further analyses are based on the interiors of the materials.

Figure 1 shows the optical microstructures of the composite samples. The morphology of the Ni particles in samples 1 and 2 is very different from that of Ni–Ti particles in samples 3 and 4. The Ni particles appear to be small rods of about 20 μm long and 2–3 μm across; some particles agglomerate together. On the other hand, the Ni–Ti particles are spheres with a diameter of about 50 μm, and the particles are distributed discretely and randomly. The difference in morphology of the metal particles originates from the starting powders and from the processing. Although both powders are sieved under 63 μm, the Ni powders are originally finer and more agglomerated than the Ni–Ti powders. During attrition milling Ni particles become rod-shaped because of the plastic deformation caused by inter-particle friction, while Ni–Ti particles are very rigid and much less influenced by milling.

The regions near the interfaces between the metal particles and ceramics have been studied by SEM. In samples 1 and 2, the interface between the Ni and Al_2O_3 is sharp. In samples 3 and 4, an interfacial reaction layer between Ni–Ti and Al_2O_3 is observed. EDS analysis indicates that the interface layer is rich in Ti, as shown in Fig. 2 which is the Ti mapping in samples 3 and 4. In sample 3, Ti is mostly concentrated at the rim of each Ni–Ti particle, while in sample 4, Ti is distributed throughout the Ni–Ti particle, although it is also enriched at the particle surfaces.

To investigate the details of the structure in the

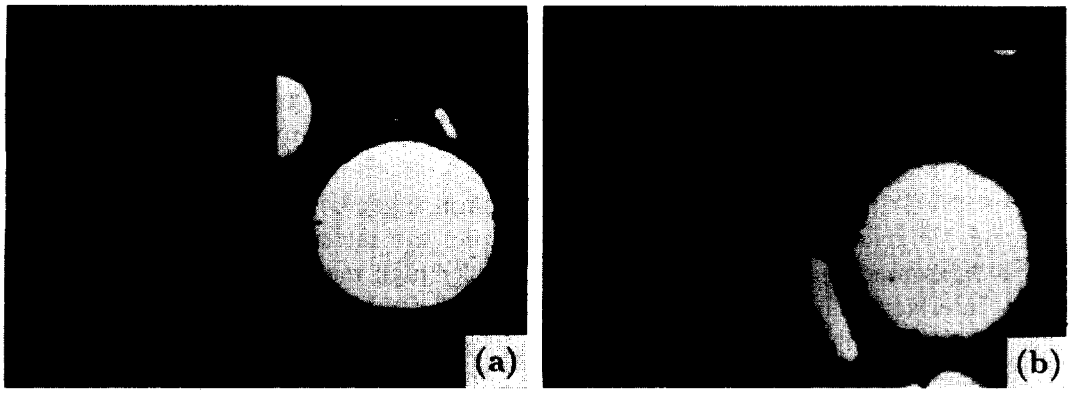

Fig. 2. Ti mapping by SEM/EDS, (a) sample 3 and (b) sample 4.

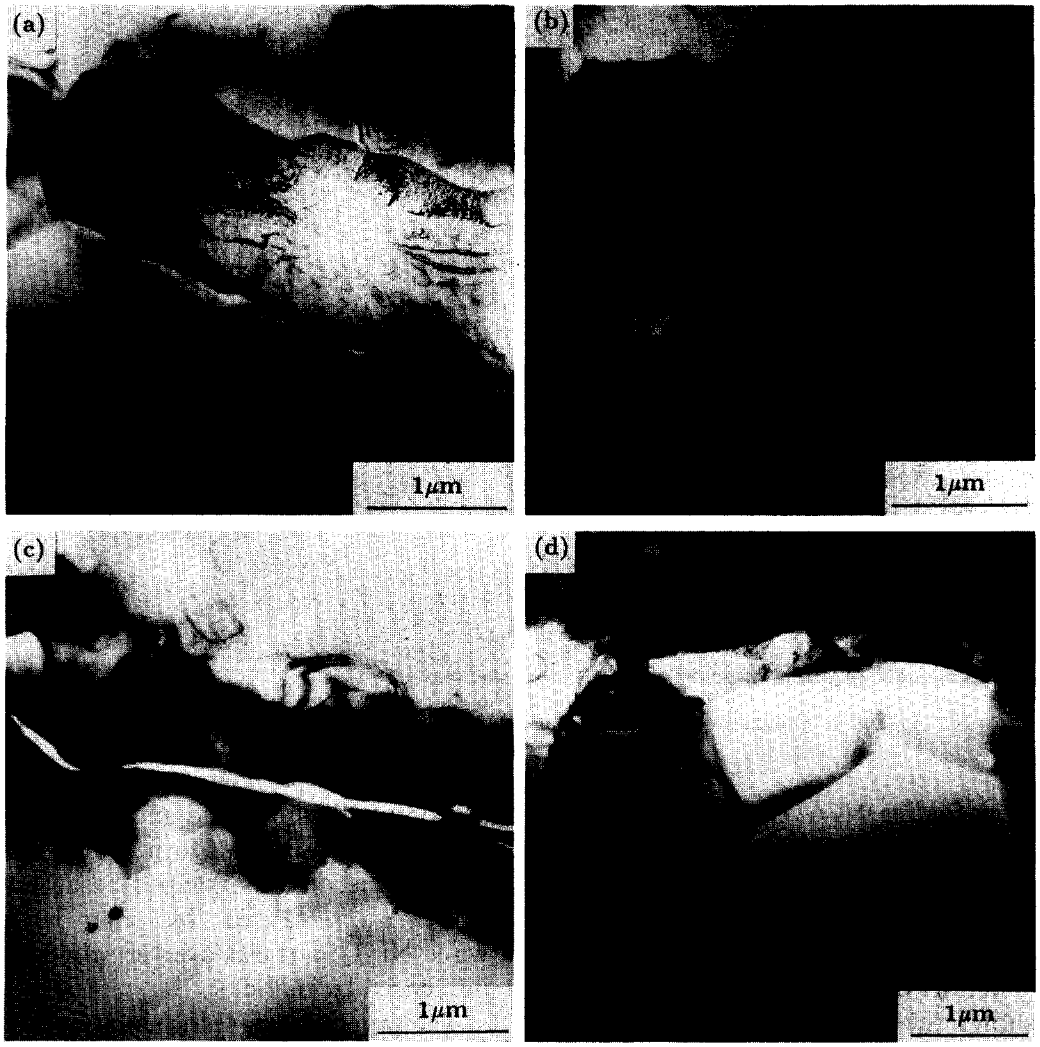

Fig. 3. TEM low magnification images which show general structures of the Ni(Ti)/Al_2O_3 interface. In (a) for sample 1 and (b) for sample 2 no interfacial layer is observed. In (c) for sample 3 and (d) for sample 4 a reaction layer can be seen.

interfacial region, TEM experiments have been carried out. Figure 3 shows the general structures around the metal particles under TEM with low magnification. In Fig. 3 (a) and (b), the bright-field images of the interfaces in samples 1 and 2, the Ni particle is surrounded by Al_2O_3 grains with an average size of about 0·6 μm, and the interface remains sharp and clear. In Fig. 3(c) and (d), an interfacial layer exists between the Ni–Ti and Al_2O_3 as also observed by SEM. On average, the layer is about 2–3 μm thick in sample 3 and about 1 μm thick in sample 4. Cracks are often observed along the interfacial regions in sample 3, within the layer as shown in Fig. 3 (c) or at the boundary between the layer and the ceramic matrix. The interfacial layer and the Ni–Ti particle are bonded very well. This indicates a relatively strong bonding between interfacial layer/metal and a relatively weak bonding between interfacial layer/ceramic. Similar interfacial behaviour is also observed by examining the details of the indentation crack path in both samples 3 and 4 under SEM.

In addition to the interfacial layer, another feature in the microstructure of the Ni–Ti/Al_2O_3 composites is the inhomogeneity of the Al_2O_3 grain size. The grains close to the interface, about 2·5 μm in sample 3 and 1·4 μm in sample 4, are much larger than the grains further away from the interface, which are, as in samples 1 and 2 (Fig. 3(a) and (b)), under 1 μm. In this study, the grain size of the monolithic Al_2O_3 is about 2·5 μm. Therefore, it can be concluded that while Ni and Ni–Ti inclusions suppress grain growth in the Al_2O_3 matrix, Ti diffusion from the Ni–Ti bulk promotes grain growth in the surrounding Al_2O_3 matrix near the interface.

To determine whether there is an interfacial reaction layer between the Ni and Al_2O_3 at a local scale, the interfaces have been analyzed by TEM under high magnification, as demonstrated in Fig. 4 (a) and (b) for a typical interface region in samples 1 and 2 respectively. Some shadowed regions along the interfaces are observed due to the projection of the interface plane which is not parallel

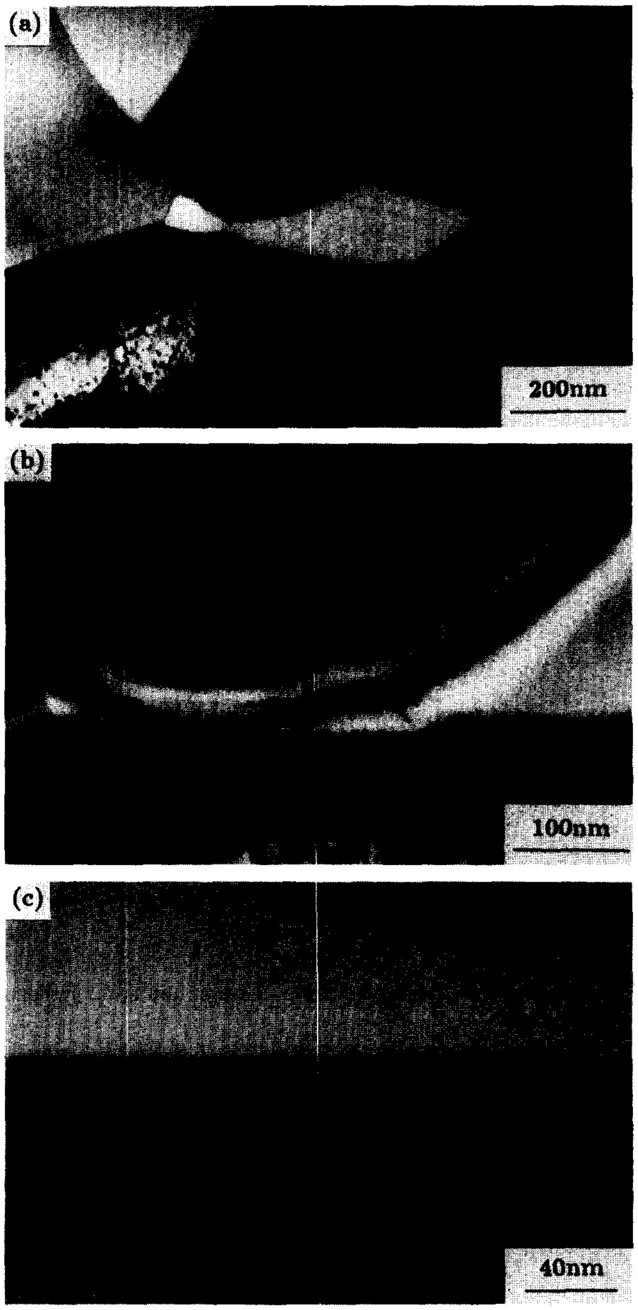

Fig. 4. High magnification TEM images of the Ni/Al_2O_3 interface, (a) sample 1, (b) sample 2; and (c) sample 1, same as (a) but at higher magnification.

to the electron beam. The interface becomes sharp and narrow when the specimen is tilted to an appropriate orientation so that the interface becomes vertical. Figure 4 (c) is a portion of the interface in sample 1 at an even higher magnification. The fringes parallel to the interface are due to the shallow interface. Apart from that there is no sign of interfacial layers or of precipitates larger than about 10 nm.

The interfacial layers in samples 3 and 4 are seen in more detail in high magnification in Fig. 5. The contrast of the interfacial layer is clearly different from that of the Ni–Ti particle and of the matrix. In Fig. 5 (a) for sample 3, some egg-shaped grains appear in the layer, and again there is a crack mainly along the boundary between the layer and the ceramic matrix. In Fig. 5 (b) for sample 4, the interfacial layer is thinner and less rich in structure than that in 3.

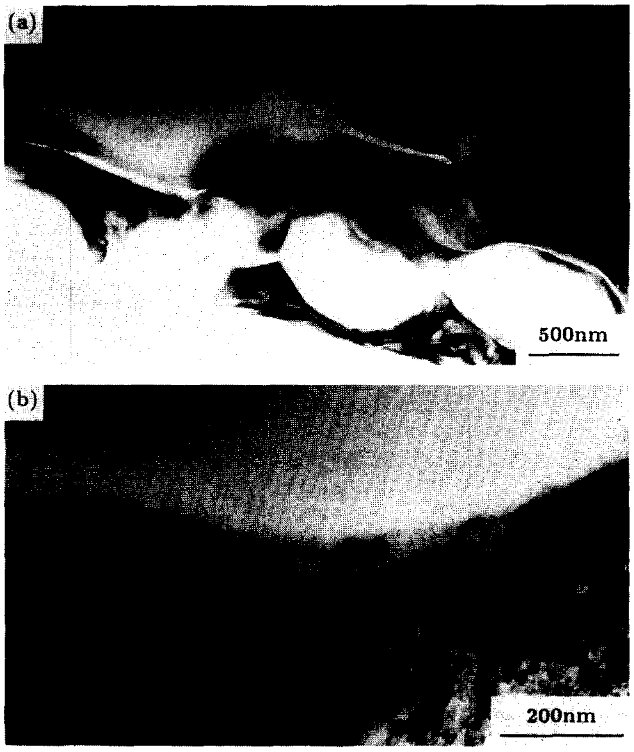

Fig. 5. High magnification TEM images of the $Ni–Ti/Al_2O_3$ interface, (a) sample 3, and (b) sample 4.

Figure 6 shows the concentration profiles of Ti, Al and Ni across an interfacial layer after a quantitative analysis by line scan from a Ni–Ti particle (left) to the Al_2O_3 matrix (right) in sample 3. In the Ni–Ti particle, Ti is almost completely depleted. In the layer, the content of Ni is very limited, and Ti is concentrated. The diffusion depth of Ti is as much as 4–5 μm into the Al_2O_3.

Semi-quantitative analysis from TEM/EDS reveals that a large amount of oxygen is present in the layers. Figure 7 (a) shows the concentration profiles after a series of analyses, and Fig. 7(b) is the corresponding TEM image with the points

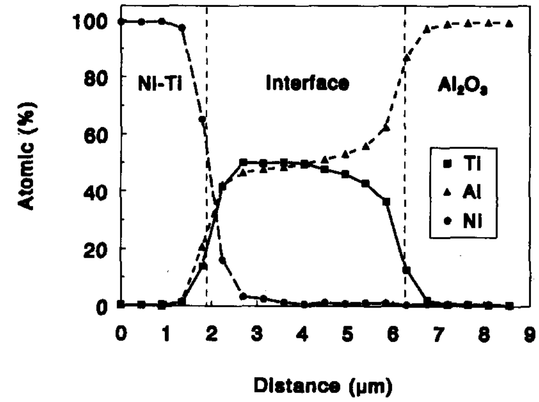

Fig. 6. Composition profile around the interface in sample 3 after a quantitative analysis by SEM/EDS with standard.

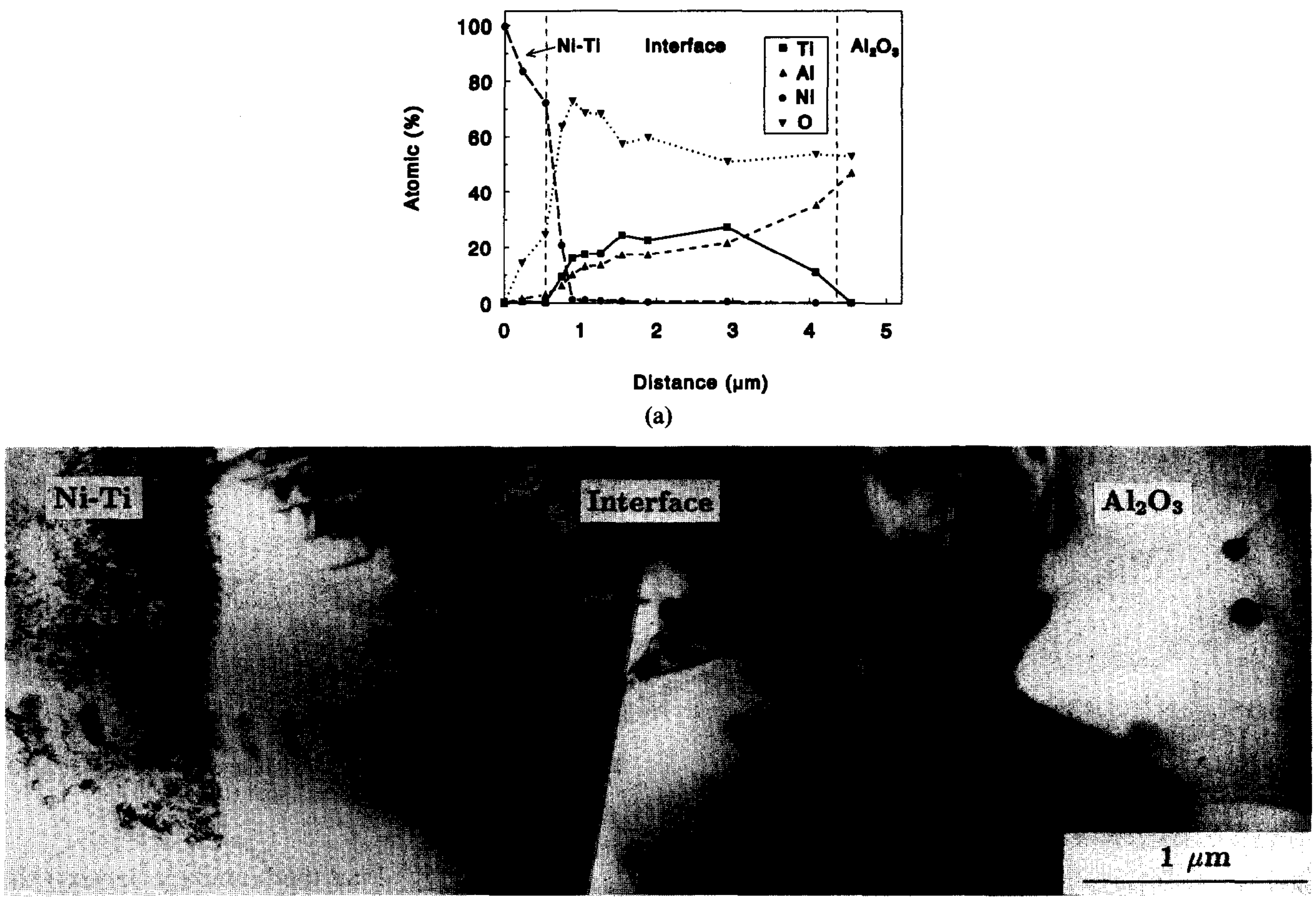

(a)

(b)

Fig. 7. (a) Composition profile in sample 3 after a semi-quantitative analysis by TEM/EDS. (b) The contamination spots indicate where the EDS analyses were taken.

where the spectra were taken indicated by the contamination spots. The high oxygen level should be treated with caution because of the nature of the semi-quantitative analysis. Some oxygen has diffused into the Ni–Ti particle to a distance of about 500 nm, associated with the diffusion of small amounts of Al. Similar to Fig. 6, Ti approaches zero in the Ni–Ti particle, but diffuses into Al_2O_3 to a distance of 4·5 μm.

The interfacial layers in sample 4 have been similarly examined. Due to the very thin thickness (only about 1 μm), the exact composition of the layer cannot be determined quantitatively. Semi-quantitative analyses by TEM/EDS indicate the presence of Ti, Al and O in the layers.

4 Analysis

4.1 Chemistry of the interface

As stated earlier, interfacial reactions play an important role in the final mechanical properties of composite materials. The probable reactions can be predicted from thermodynamic data.[10] In the Ni/Al_2O_3 system, the possible reactions are the formation of NiO or $NiAl_2O_4$ spinel. For the reaction

$$2Ni + O_2 \longrightarrow 2NiO \qquad (1)$$

$\Delta G = -198{\cdot}2$ kJ and the equilibrium oxygen partial pressure is 5×10^{-7} bar at 1400°C. As soon as NiO is formed, reaction with Al_2O_3 will proceed to develop $NiAl_2O_4$ spinel, because the reaction

$$NiO + Al_2O_3 \longrightarrow NiAl_2O_4 \qquad (2)$$

with $\Delta G = -18{\cdot}5$ kJ has a negative Gibbs energy at 1400°C.

However, direct formation of $NiAl_2O_4$ spinel between Ni and Al_2O_3 is also possible as illustrated in Ni/Al_2O_3 diffusion couples and diffusion bonding experiments.[11-13] The formation of $NiAl_2O_4$ spinel at Ni/Al_2O_3 interfaces need not proceed through a NiO intermediate, but requires a threshold activity of oxygen dissolved in Ni, which is less than the solubility limit of oxygen in Ni in equilibrium with NiO. The threshold oxygen level is 0·025 at% (250 ppm) at 1400°C from thermodynamic calculation.[13]

In the present work, the oxygen level in the CO atmosphere is estimated to be 3×10^{-17} bar in equilibrium conditions (calculated from the oxidation of C to CO at 1400°C). Comparing this value with the equilibrium oxygen partial pressure for

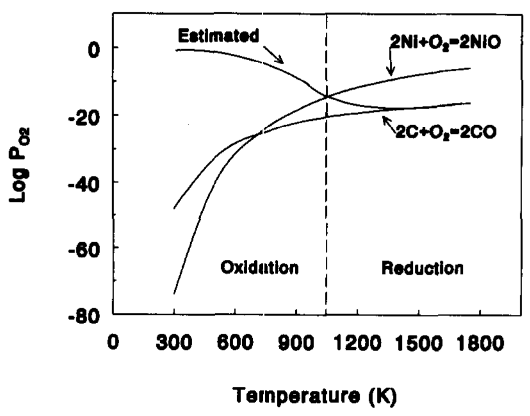

Fig. 8. Oxygen level estimated in the CO sintering atmosphere during heating.

Ni oxidation, 5×10^{-7} bar, it appears that NiO formation in the CO atmosphere is not predicted. Therefore spinel formation should not arise through a NiO precursor. On the other hand, direct spinel formation is also not predicted because the oxygen content in the Ni is very limited in the raw material (99·99 + %). In the case of Ar atmosphere, the oxygen partial pressure is expected to be 3×10^{-6} bar. Ni should then be oxidized and $NiAl_2O_3$ should be also formed subsequently. These estimations do not completely agree with the experimental observations, which show that both NiO and $NiAl_2O_4$ spinel are present on the surfaces, but not in the interiors of all the samples sintered in both atmospheres. The difference can be attributed to the real oxygen level during heating. The CO atmosphere is generated by burning C powder in a closed crucible, so that the oxygen level decreases from 0·21 bar in the initial air to as low as 3×10^{-17} bar at 1400°C under equilibrium conditions. This process is shown schematically in Fig. 8. During the initial period of heating, the oxygen level is high enough for Ni oxidation and $NiAl_2O_4$ formation. The oxide and spinel formed can be reduced again at higher temperatures when the oxygen level approaches the equilibrium one. This has been supported in our experiments by extending the holding time at 1400°C. The surface NiO and $NiAl_2O_4$ spinel layer is observed to diminish. In both atmospheres, oxygen is consumed gradually. Penetration of the oxygen into the interior of the samples is probably too limited to make Ni oxidized there. The initial oxygen enclosed in the powder compacts (green bodies) alone cannot cause prominent Ni oxidation. Provided that all the oxygen in the interior is consumed to produce NiO, a layer as thin as about 3 Å is estimated on surfaces of the Ni particles, which cannot be detected by TEM analysis. In fact, some of the oxygen may be dissolved in Ni, making the NiO layer even thinner.

In the Ni–Ti/Al_2O_3 composites, the interfacial layer contains only Ti, Al and O, and Ni is much less involved. Apparently, Ti diffuses from the interior of the Ni–Ti particles to the particle surfaces, and then the Ti at the particle surfaces reacts further with oxygen and the Al_2O_3 matrix.

From the phase diagram of the Ti–O system,[14] Ti can dissolve a large amount of oxygen and can be very easily oxidized to form a family of oxides such as TiO, Ti_2O_3, TiO_2 and so on. Considering the following reactions

$$Ti + 1/2O_2(g) \rightarrow TiO \qquad \Delta G = -382\ \text{kJ} \quad (3)$$

$$Ti + 3/4O_2(g) \rightarrow 1/2Ti_2O_3 \qquad \Delta G = -534\ \text{kJ} \quad (4)$$

$$Ti + O_2(g) \rightarrow TiO_2 \qquad \Delta G = -642\ \text{kJ} \quad (5)$$

and the activity of 6 at% Ti in Ni, estimated to be $2{\cdot}6 \times 10^{-4}$ at 1400°C,[15] the equilibrium oxygen partial pressures for the above reactions are $2{\cdot}1 \times 10^{-17}$, $3{\cdot}5 \times 10^{-18}$ and $3{\cdot}5 \times 10^{-17}$ bar, respectively. Because of the high oxygen level in both sintering atmospheres (especially high during heating in the CO atmosphere as indicated from the Ni/Al_2O_3 surface reactions), Ti can be easily oxidized. The oxide is probably in the form of TiO_2 (rutile), since experiments on the Ni–Ti powders treated in CO atmospheres similar to those of the sintering conditions show that a layer of TiO_2 (rutile) is present on the surface of each Ni–Ti particle. The titanium oxide at the Ni–Ti/Al_2O_3 interface can dissolve into the Al_2O_3 and promote Al_2O_3 grain growth.[16] The thicker reaction layer in the CO atmosphere than in the Ar atmosphere is attributed to the higher oxygen level in the former case during the heating stage. The formation of TiC is not possible from thermodynamic considerations.

4.2 Relationship between structure and properties

From the fracture surface analyses and from the indentation crack path examinations, it is found that the Ni or Ni–Ti metallic particles do not undergo substantial plastic stretching as a crack tip passes by. Cracks propagate mainly along the interface between the metal inclusions and the Al_2O_3 ceramic. The toughening mainly comes from the crack deflection instead of from the desired plastic stretching of the metal. Because crack deflection is relatively ineffective in toughening,[17] this explains the small improvement in the toughness of the composites. As to the low fracture strength of the composite compared to monolithic Al_2O_3, this is due to defects introduced by the metal inclusions (which themselves can be taken as flaws) and to the influence of the sintering atmospheres. Contamination from C due to the CO atmosphere may be responsible for the specially low strength of the composites sintered in CO. As is known, C is detrimental to the mechanical properties of alumina.[18]

For samples 1 and 2, the difference in microstructure and interface is hardly detectable. The difference in fracture toughness can be attributed to the ductility of Ni. In sample 1, the absorption of C from the atmosphere make the Ni particles more resistant to yield,[19] hence providing a lesser contribution to the toughening. For samples 3 and 4, the negative influence of the Ni–Ti inclusions on the fracture toughness is related to the weak interfacial layer and boundary between the layer and the Al_2O_3 matrix. Cracks occur at the interface resulting from the stress of thermal expansion mismatch between the large metal particles and the matrix. So the metal particles may act to some extent as pores. The weak interface debonding releases only very little energy to resist the crack propagation. Furthermore, titanium does not only modify the interface structure but also changes the yield strength of the Ni particles, which makes the plastic stretching of the metal particles even more difficult.

5 Conclusions

Ni/Al_2O_3 and $Ni–Ti/Al_2O_3$ composites have been fabricated by sintering in CO and Ar atmospheres. All the samples are well densified after sintering at 1400°C. The fracture toughness is not much improved compared with the matrix because of the very limited plastic stretching of the metal particles. Argon atmosphere is found to be beneficial to the mechanical properties relative to CO atmosphere for all the composites. In both sintering atmospheres no interfacial reaction layers are formed in the Ni/Al_2O_3 composites; in contrast there are reaction layers up to 1–3 μm in thickness in the $Ni–Ti/Al_2O_3$ composites. The reaction is due to the oxidation of Ti, and is more accelerated in CO atmosphere than in Ar. As expected, Ti diffuses from the interior of Ni–Ti alloy particles to the particle interfaces, but the weak interfacial layer and the poor bonding between the layer and the matrix result in materials which are not toughened.

Acknowledgement

The authors gratefully acknowledge the suggestions and criticism provided by Prof. R. J. Brook and Prof. F. J. J. van Loo during the experimental work and preparation of the manuscript.

References

1. Sigl, L. S., Mataga, P. A., Dalgleish, B. J., & Mcmeeking, R. M., On the toughness of brittle materials reinforced with a ductile phase. *Acta Metall.*, **36** (1988) 945–53.
2. Ashby, M. F., Blunt, F. J. & Bannister M., Flow characteristics of highly constrained metal wires. *Acta Metall.*, **37** (1989) 1847–57.
3. Flinn, B. D., Rühle, M. & Evans, A. G., Toughening in composites of Al_2O_3 reinforced with Al. *Acta Metall.*, **37** (1989) 3001–6.
4. Lu, T. C., Evans, A. G., Hecht, R. J. & Mehrabian, R., Toughening of $MoSi_2$ with a ductile (niobium) reinforcement. *Acta Metall. Mater.*, **39** (1991) 1853–62.
5. Chen Z. & Mecholsky, J. J., Jr, Control of strength and toughness of ceramic/metal laminates using interface design. *J. Mater. Res.*, **8** (1993) 2362–9.
6. Tuan, W. H. & Brook, R. J., The toughening of alumina with nickel inclusions. *J. Eur. Ceram. Soc.*, **6** (1990) 31–7.
7. Sun, X. & Yeomans, J. A., The toughening of alumina matrices by the inclusion of nickel particles. *Special Ceramics*, **9**, 1990.
8. Nicholas, M. G. & Crispin, R. M., Brazing ceramics with alloys coating titanium. *Ceram. Eng. Sci. Proc.*, **10** (1989) 1602–12.
9. Armstrong, W. M., Chaklader, A. C. D. & Clarke, J. F., Interface reactions between metals and ceramics: I. Sapphire-nickel alloys. *J. Am. Ceram. Soc.*, **45** (1962) 115–18.
10. SGTE (Scientific Group Thermodata Europe) Substance Data Files, Thermodata GmbH, Grenoble University, St martin d'heres, France, 1987.
11. Backhaus-Ricoult, M., Diffusion process and interphase boundary morphology in ternary metal–ceramic systems. *Ber. Bunsenges. Phys. Chem.*, **90** (1986) 684–90.
12. Metselaar, R. & Van Loo, F. J. J., The use of phase diagrams for the study of metal–ceramic interdiffusion. In *Ceramic Developments*, Vols. 34–36. ed. C.C. Sorrel & B. Ben-Nissan, *Materials Science Forum*, 1988, pp. 413–20.
13. Trumble, K. P. & Rühle, M., The thermodynamics of spinel interphase formation at diffusion-bonded Ni/Al_2O_3 interfaces. *Acta Metall. Mater.*, **39** (1991) 1915–24.
14. Murray, J. L. & Wriedt, H. A., The O–Ti (oxygen–titanium) system. *Phase Diagrams of Binary Titanium Alloys*, 1987.
15. Murray, J. L., The Ni–Ti (nickel–titanium) system. *Phase Diagrams of Binary Titanium Alloys*, 1987.
16. Tsui, Y.-P. & Johnson, D. L., Influence of TiO_2 and Fe_2O_3 on the densification of Al_2O_3. In *Proc. Int. Symp. of Factors in Densification and Sintering of Oxide and Non-Oxide Ceramics*, Japan, 1978.
17. Faber, K. T. & Evans, A. G., Crack deflection processes —I. Theory. *Acta Metall.*, **31** (1983) 565–76.
18. Döre, E. & Hübner, H., *Alumina, Processing, Properties, and Applications*. Springer-Verlag, Berlin, 1984.
19. Ross, R. B., *Metallic Materials Specification Handbook*, 3rd Edn. E. & F. N. Spon Ltd, London, 1980, pp. 227–8.